ISBN 2447-6102

Article

Numerical simulation of thermofluid-dynamics over isothermal cylinders *in tandem* using the immersed boundary method

Rômulo Damasclin Chaves dos Santos, Ph.D. [1]

1 *Substitute Professor of Mathematics at the Federal Institute of Education, Science and Technology of Acre, Brazil. Av. Brasil, 920, Xavier Maia, Rio Branco-AC, CEP 69.903-068.*

E-mail: romulo.santos@ifac.edu.br

Recebido: 12/01/22; Aceito: 13/12/22; Publicado: 31/01/23

Abstract: This work presents an Immersed Boundary Method (IBM) for the study of fluid-body interaction in two-dimensional thermofluidynamics. The method is applied to the study of heat-transfer by forced convection and onset turbulence around isothermal cylinders in tandem, immersed in an incompressible Newtonian fluid. The fluid motion and temperature are defined on a Lagrangian mesh, and a Virtual Physical Model is used to impose the no-slip boundary condition and evaluate the heat exchange between the fluid and the solid surface. The Navier-Stokes and energy equations are solved under physically appropriate boundary conditions. The onset turbulence is modeled using the Smagorinsky Model, and the results show that recirculation increases with increasing Reynolds number and decreases with increasing Richardson number, and also the thermal plumes moving upwards are generated. The results are validated with previous numerical results for different Reynolds numbers.

Keywords: Forced Convection; Immersed Boundary Method; Smagorinsky Model.

1. Introduction

Many physical phenomena in fluid mechanics can be described mathematically through the use of a set of nonlinear partial differential equations, known as the laws of conservation of fluid mechanics. These laws include conservation of momentum, conservation of mass (also known as continuity), and conservation of energy. Together, these laws model the dynamics of the forces acting on the fluid, as well as, the energy exchange that occurs in different regions of the flow. In this work, these equations were discretized using the finite difference method for an incompressible Newtonian fluid, which relates the term of viscous stress to the deformation rates in the velocity field, thus simulating the flow dynamics using the Navier-Stokes equations.

Traditional methods of domain discretization can be difficult to implement and require significant computation time, often necessitating the use of successive remeshing processes and the introduction of new generalized coordinate systems. In order to address these challenges, a computational code was developed for the immersed boundary methodology for the study of thermofluidynamics interactions. This work presents some of the main studies involving the IBM, specifically focusing on the heat-transfer by mixed convection process. The purpose of these references is to provide a theoretical foundation for the methodology, highlighting important physical and mathematical concepts that will be applied in the current work.

Among the main reference involving the thermal part, we can list some important ones, such as, Badr & Dennis (1985) and Badr et al. (1990). These works do not present the IBM, but they are an excellent precursor in relation to the flow around rotating circular cylinder involving forces convection, being the theoretical basis used in other important works for the implementation of the thermal part. In summary, the experimental and numerical works of the authors Badr & Dennis considering the problem of laminar flow with heat-transfer by forced convection from a rotating circular cylinder around its own axis, initially for a Reynolds number equal to 100, with a specific rotation rate (α) for the interval varying between $(0.5 \leq \alpha \leq 3.0)$. Meanwhile, the second work, uses the Reynolds numbers range varying between $(10^3 \leq Re \leq 10^4)$, with specific rotation rate equal to 4.0. In both works, the cylinder is located in a uniform flow. Thus, the author report that the temperature fields are strongly influence by the vorticity of rotation of the cylinder. The authors found, in both studies, that the heat-transfer coefficient tends to decrease as the rotation of the cylinder increase. An attribution of the presence of a layer of the rotation around the cylinder was verifying, being separated from the main fluid of the flow. Thus, the results demonstrated convergence and numerical stability compared to others available in the literature (see, Lai & Peskin (2006) and Sharma et al. (2012)).

Ashrafizadeh and Hosseinjani (2017) present an extension of the Immersed Boundary Method (IBM) for the analysis of natural and mixed convection processes in a two-cylinder side-by-side configuration with alternating rotation velocity and heating. The study is conducted in a cold and square cavity containing air, with a Prandtl number (Pr) of 0.7. The study explores the effect of varying rotation rates and different values of Rayleigh and Richardson numbers. Pure natural convection cases are also considered. The study includes an examination of isothermal lines, streamlines, Nusselt numbers, and local and average heat transfer around the solid boundary. The IBM is used to handle the boundary conditions and solve the governing equations for a two-dimensional flow, using an orthogonal Cartesian mesh.

Santos et al. (2018) presented an application of the Immersed Boundary Method (IBM) for low and high Reynolds numbers, coupled with the Virtual Physical Model (VPM) proposed by Silva et al. (2003) to calculate the Lagrangian forced field, based only on the momentum equation. The study simulates two-dimensional incompressible flows around a heated square cylinder, with the temperature considered constant at the surface. The results showed a good numerical agreement, with the margin of error being less than 3% when compared to other works. The study also obtained the temporal evolution of the drag and lift coefficients, as well as the Nusselt number, using the same methodology and parameters obtained from Eulerian fields. The study also noted that the geometry used in this work presents singularities, which were taken into account in the construction of the root algorithm (computational code), making it applicable to other geometries. Additionally, the results showed that the influence of the surface of the heated body immersed in the flow increases as the Reynolds number increases. A turbulence model was also used to model the energy transfer process between the largest and smallest turbulent scales.

Santos and Gama (2021) presented an investigation of the thermal and turbulence behaviors of incompressible Newtonian flow by numerical simulation. The study combines two physical phenomena, namely heat-transfer by natural and forced convection and onset of turbulence, around different isothermal complex geometries using the IBM to model the presence of the isothermal body. The study implements boundary conditions of the Dirichlet and Neumann types. For turbulence modeling, the Smagorinsky and Spalart-Allmaras models are used for Reynolds and Richardson numbers ranging up to 5000 and 5, respectively. The authors confirm that downstream of the immersed body, recirculation: i) increases with the increase in Reynolds number while keeping the Richardson number constant, ii) decreases with the increase in Richardson number while preserving the Reynolds number constant. They also confirm the generation of thermal plumes moving upwards. iii) For Reynolds numbers in the order of a few hundred and Richardson numbers around 5, the study observed the formation of vortex wake in the downstream region for tandem cylinders. iv) Interactions within the vortex wake, with the shear layer separated from the downstream cylinder, create two vortices near the downstream cylinder. v) The shear layer separating from the upstream cylinder creates a vortex behind the downstream cylinder.

In this work, constant properties are considered. The buoyancy term is based on the Boussinesq approximation, which is used to model forced convection. Other terms, such as energy generation and internal heat or humidity, are neglected, as well as, the effects of Coriolis forces or rotation. The proposed methods were validated for forced convection in an isothermal body geometry. By combining the forced convection heat-transfer with the onset turbulence model considered in this work, the methodology is validated around the immersed isothermal body (cylinders *in tandem*). The next section presents the mathematical methodology.

2. Mathematical methodology

2.1 Formulation for the fluid motion and temperature

Consider an incompressible viscous flow in a two-dimensional domain that contains a domain Ω and border $\partial\Omega_b$, being heated with isothermal temperature (or constant temperature on the surface of the immersed body) modelled through discretized (Lagragian) points. As in previous studies, a forcing term is included in the momentum equations, and a heat source term is incorporated into the energy equation. As a result, the governing equations that describe mixed convection (dimensional and primitive form) can be written in primitive variable forms as follows:

$$\boldsymbol{\rho_0}\left(\frac{\partial \boldsymbol{u}}{\partial \boldsymbol{t}}+(\boldsymbol{u}\cdot\nabla)\boldsymbol{u}\right)=-\nabla \boldsymbol{p}+\boldsymbol{\mu}\nabla^2\boldsymbol{u}+\boldsymbol{f}, \tag{1}$$

$$\boldsymbol{\rho_0}\left(\frac{\partial \boldsymbol{u}}{\partial \boldsymbol{t}}+(\boldsymbol{u}\cdot\nabla)\boldsymbol{u}\right)=-\nabla \boldsymbol{p}+\boldsymbol{\mu}\nabla^2\boldsymbol{u}+\boldsymbol{\rho_0 g}\big(\boldsymbol{1}-\boldsymbol{\beta}(\boldsymbol{T}-\boldsymbol{T_\infty})\big)\boldsymbol{j}+\boldsymbol{f}, \tag{2}$$

$$\boldsymbol{\rho_0 c_p}\left(\frac{\partial \boldsymbol{T}}{\partial \boldsymbol{t}}+(\boldsymbol{u}\cdot\nabla)\boldsymbol{T}\right)=\boldsymbol{k}\nabla^2\boldsymbol{T}+\boldsymbol{q}, \tag{3}$$

$$\nabla\cdot\boldsymbol{u}=\boldsymbol{0}, \tag{4}$$

where Eqs. (1), (3) and (4) are for forced convection, while Eqs. (2), (3) and (4) are for natural convection (in Eq. (2), the Boussinesq approximation is used), the set of these equations form the heat transfer process by mixed convection. The symbols (*i*) $\boldsymbol{u},\boldsymbol{p},\boldsymbol{T}$ and $\boldsymbol{T_\infty}$ denote velocity vector, pressure, temperature and reference temperature, respectively; *(ii)* $\boldsymbol{\rho_0}$, $\boldsymbol{\mu}$, $\boldsymbol{\beta}$, $\boldsymbol{k}$ and $\boldsymbol{c_p}$ are, fluid density at temperature, viscosity, thermal diffusivity, thermal expansion coefficient specific heat at constant pressure, respectively; *(iii)* $\boldsymbol{g}$ is a downward gravitational acceleration, *(iv)* the therm $\boldsymbol{\rho_0 g\beta}(\boldsymbol{T}-\boldsymbol{T_\infty})$ accounts for the effects of the fluid temperature on the fluid flow, and *(v)* $\boldsymbol{j}$ is the unit vector in the positive y-axis direction, respectively.

The governing equations are dimensionless by using characteristics scales such as the fluid density $\boldsymbol{\rho_0}$ for the characteristic density, the far-field velocity $\boldsymbol{U_\infty}$ for the characteristic velocity, and the body diameter $\boldsymbol{D}$ for the characteristic length. The following characteristic scale are introduced: $\boldsymbol{D}/\boldsymbol{U_\infty}$ for time; $\boldsymbol{\rho_0}\,\boldsymbol{U_\infty^2}/\boldsymbol{D}$ for de Eulerian *momentum* force or simply forcing term, represented by $\boldsymbol{f}$. To reduce the calculation process, the Momentum Eq. (1), and Energy Eq. (3) equations, are rewritten in dimensionless form, represented by the equations:

$$\frac{\partial \boldsymbol{u}}{\partial \boldsymbol{t}}+(\boldsymbol{u}\cdot\nabla)\boldsymbol{u}=-\nabla \boldsymbol{p}+(\boldsymbol{Re})^{-1}\nabla^2+\boldsymbol{Gr}(\boldsymbol{Re})^{-2}\boldsymbol{gT}\;+\boldsymbol{f}, \tag{5}$$

$$\left(\frac{\partial \boldsymbol{T}}{\partial \boldsymbol{t}}+(\boldsymbol{u}\cdot\nabla)\boldsymbol{T}\right)=(\boldsymbol{Re}\cdot\boldsymbol{Pr})^{-1}+\boldsymbol{q}, \tag{6}$$

where $\boldsymbol{Re}$ is the Reynolds number, defined mathematically by $\boldsymbol{Re}=\boldsymbol{\rho_0 U_\infty D}/\boldsymbol{\mu}$, and $\boldsymbol{Gr}$ is the Grashof number, defined by $\boldsymbol{Gr}=\boldsymbol{g\beta}(\boldsymbol{T}-\boldsymbol{T_\infty})\boldsymbol{D^3}/\boldsymbol{\nu^2}$. The therm $\boldsymbol{Pr}$, denotes the Prandtl number, defined by $\boldsymbol{Pr}=\boldsymbol{\nu}/\boldsymbol{\alpha}$, where $\boldsymbol{\alpha}$ and $\boldsymbol{\nu}$ are the thermal diffusivity and kinematic viscosity, respectively. With regard to the dimensionless continuity equation, it assumes the same form as the dimensional continuity equation.

The forcing term $\boldsymbol{f}$ in the momentum Eqs. (1) and (2) is the force density at the fluid (Eulerian mesh) points distributed from the force density at the boundary (Lagrangian) point, which can be expressed as

$$\boldsymbol{f}(\boldsymbol{x},\boldsymbol{t})=\int_{\partial\Omega_b}\mathbf{F}\,(\boldsymbol{X_k},\boldsymbol{t})\boldsymbol{\delta}(\boldsymbol{x}-\boldsymbol{X_k})\boldsymbol{dX_k}\,, \tag{7}$$

where $\boldsymbol{F}(\boldsymbol{X_k},\boldsymbol{t})$ is the Lagrangian force density, calculated on the interface points $\boldsymbol{x}$ and $\boldsymbol{X_k}$ which are the position vectors of the Eulerian and Lagragian points, respectively. The presence of the Dirac delta function, $\boldsymbol{\delta}(\boldsymbol{x}-\boldsymbol{X_k})$, represents the interaction between the fluid and the immersed boundary.

Similarly, the thermal source, represented by $\boldsymbol{q}$, is added to Eq. (3), being responsible for making the flow feel the presence of the heat solid interface, being expressed by

$$\boldsymbol{q}(\boldsymbol{x},\boldsymbol{t}) = \int_{\partial\Omega_b} \mathbf{Q}\,(\boldsymbol{X_k},\boldsymbol{t})\boldsymbol{\delta}(\boldsymbol{x}-\boldsymbol{X_k})\boldsymbol{dX_k}\,, \tag{8}$$

where $\boldsymbol{Q}(\boldsymbol{X_k},\boldsymbol{t})$ is the (virtual boundary) heat flux on the Lagrangian point, $\boldsymbol{X_k}$.

2.2 Dimensionless equations for mixed convection

Thus, the implicit calculation for the dimensional equations (1)-(4), is performed in a dimensionless way with the following equations:

$$\boldsymbol{D_t U} = -\boldsymbol{\nabla p} + (\boldsymbol{Re})^{-1}\boldsymbol{\nabla^2 U} + \int_{\Gamma} \mathbf{F}\,(\boldsymbol{X_k},\boldsymbol{t})\boldsymbol{\delta}(\boldsymbol{x}-\boldsymbol{X_k})\boldsymbol{dX_k}, \tag{9}$$

$$\boldsymbol{D_t U} = -\boldsymbol{\nabla p} + (\boldsymbol{Re})^{-1}\boldsymbol{\nabla^2 U} + \boldsymbol{Gr}(\boldsymbol{Re})^{-2}\boldsymbol{\Theta j} + \int_{\Gamma} \mathbf{F}\,(\boldsymbol{X_k},\boldsymbol{t})\boldsymbol{\delta}(\boldsymbol{x}-\boldsymbol{X_k})\boldsymbol{dX_k}, \tag{10}$$

$$\boldsymbol{D_t \Theta} = (\boldsymbol{Pe})^{-1}\boldsymbol{\nabla^2 \Theta} + \int_{\Gamma} \mathbf{Q}\,(\boldsymbol{X_k},\boldsymbol{t})\boldsymbol{\delta}(\boldsymbol{x}-\boldsymbol{X_k})\boldsymbol{dX_k}, \tag{11}$$

$$\boldsymbol{\nabla}\cdot\boldsymbol{U} = \boldsymbol{0}, \tag{12}$$

where $\boldsymbol{D_t} * = \boldsymbol{\partial_t} * + (\boldsymbol{U}\cdot\boldsymbol{\nabla}) *$ is the material derivative, $\boldsymbol{U},\boldsymbol{p}$ and $\boldsymbol{\Theta}$ are the dimensionless velocity, pressure and temperature fields, respectively. In this work, we will also refer to the Richardson number by $\boldsymbol{Ri} = \frac{\boldsymbol{g\beta(T_c - T_\infty)D}}{\boldsymbol{u_\infty^2}}$, which express the ratio between natural and forced convection, and the therm $\boldsymbol{T_c}$ is the boundary/wall temperature.

3. Mathematical modeling of turbulence

Before discussing the turbulence model, it is important for the reader to have a basic understanding of numerical methods. For more information on the Virtual Physical Model, as well as, the specific numerical methods used to calculate the coupling between velocity, pressure, and temperature, the calculation of the Lagrangian force distribution, and the thermal source, please refer to Silva et al. (2003) and Santos & Gama (2021).

3.1. Smagorinsky model

The Smagorinsky algebraic model (1963) is built on the assumption of local equilibrium for small scales, meaning that the energy input into the spectrum is equal to the energy dissipated by viscous effects. This model provides a useful tool for understanding and predicting small-scale dynamics in fluid systems. This model is based on the formulation:

$$\boldsymbol{v_t = (C_s \ell)^2 \sqrt{2\bar{S}_{ij}\bar{S}_{ij}}}\,, \tag{13}$$

where, $\bar{S}_{ij} = \frac{1}{2}\left(\frac{\partial \bar{u}_i}{\partial x_i} + \frac{\partial \bar{u}_j}{\partial x_i}\right)$ is the stress rate, ℓ is the length of the sub-mesh, and C_s is the Smagorinsky constant. The application of the damping function in the Smagorinsky method aims to reduce turbulent viscosity near the walls of the immersed boundary, regardless of the geometry being considered. For further information, refer to Smagorinsky (1963) and Santos & Gama (2021).

4. Numerical method

In this paper, was used the Fractional Steps Numerical Method (FSNM) to solve the Navier-Stokes equation, resulting in new velocity and pressure fields. The time discretization used is the first-order Euler's method, and the Navier-Stokes equation is solved implicitly. The pressure correction is done through the linear system, which is solved using the Modified Strongly Implicit Procedure, developed by Schneider and Zedan (1981). The Eq. (1) can be re-expressed as follows:

$$\boldsymbol{\frac{u_i^{n+1} - u_i^n}{\Delta t} + \left[\frac{\partial}{\partial x_j}\left(u_i^n u_j^n\right)\right] = -\frac{1}{\rho}\frac{\partial p^{n+1}}{\partial x_i} + \frac{\partial}{\partial x_j}\left[(v + v_t)\left(\frac{\partial u_i^n}{\partial x_j} + \frac{\partial u_j^n}{\partial x_i}\right)\right] + f_i^n}\,, \tag{14}$$

In the FSNM, the velocity, the pressure and the forcing term of the predictive instant, n, are used to calculate, in the predictive step, an estimate for the velocity in the current time $\bar{u}_i^{n+1}$, offered by equation

$$\boldsymbol{\frac{\bar{u}_i^{n+1} - u_i^n}{\Delta t} + \left[\frac{\partial}{\partial x_j}\left(u_i^n u_j^n\right)\right] = -\frac{1}{\rho}\frac{\partial p^{n}}{\partial x_i} + \frac{\partial}{\partial x_j}\left[(v + v_t)\left(\frac{\partial u_i^n}{\partial x_j} + \frac{\partial u_j^n}{\partial x_i}\right)\right] + f_i^n}\,. \tag{15}$$

The next step in the FSNM is to subtract Eq. (14) from Eq. (15), resulting in

$$\boldsymbol{\frac{\bar{u}_i^{n+1} - u_i^n}{\Delta t} = \frac{1}{\rho}\frac{\partial}{\partial x_i}\left(p^{n+1} - p^n\right)}\,, \tag{16}$$

performing some algebraic manipulations, the calculated pressure field is obtained, thus obtaining the corrected equation for the velocity in the current iteration (corrector step), being represented by

$$\boldsymbol{u_i^{n+1} = \bar{u}_i^{n+1} - \frac{\Delta t}{\rho}\frac{\partial p'^{n+1}}{\partial x_i}}, \tag{17}$$

where, $p'^{n+1} = p^{n+1} - p^n$.

Knowing that the velocity field must satisfy the continuity equation, one obtains

$$\boldsymbol{\frac{1}{\Delta t}\frac{\partial \bar{u}_i^{n+1}}{\partial x_i} = \frac{1}{\rho}\frac{\partial^2 p'^{n+1}}{\partial x_i \partial x_i}}\,, \tag{18}$$

Where the Eq. (18) is a Poisson equation for the correction of pressure, p'. More details about this numerical method, see Santos et al. (2018) and Santos and Gama (2021).

4.1 – The Fractional Step Method Algorithm

This algorithm consists in carrying out the following steps:

i) Estimate the velocity field, Eq. (14);

ii) With the estimated velocity field, solve the linear system for the pressure correction, Eq. (18);

iii) Correct the velocity field, Eq. (17), and pressure p'^{n+1};

iv) Check the conservation of mass within the specified tolerance;

v) Advance to the next time step.

5. Results

5.1 Generalities related to numerical simulation and additional information about the result

The IBM, implemented in C++ code, allowed the simulation of two-dimensional flows around a heated body with constant temperature that is immersed in the flow. This method took into account different Reynolds numbers. In this specific case, the simulation focuses on the flow around a pair of circular cylinders heated *in tandem* configuration, which have equal diameters and the same center-to-center distance, represented by Lcc, see Fig. (**1**). The fluid and the heat flow are characterized by Reynolds number ($\boldsymbol{Re} = {}^{\boldsymbol{\rho U_\infty D}}/_{\boldsymbol{\mu}}$), Prandtl number ($\boldsymbol{Pr} = {}^{\boldsymbol{\mu c_p}}/_{\boldsymbol{k}}$), where $\boldsymbol{\rho}$ is the fluid density, $\boldsymbol{U_\infty}$ is the free stream velocity, $\boldsymbol{D}$ is the cylinder diameter, $\boldsymbol{\mu}$ is the dynamic viscosity, $\boldsymbol{c_p}$ is heat at constant pressure and $\boldsymbol{k}$ the thermal diffusivity. In this work, numerical simulations are conducted for different Reynolds numbers, $\boldsymbol{Re = 100 - 500}$, while keeping the Prandtl number fixed at $\boldsymbol{Pr = 0.7}$ (same as the air). Both fluid flow characteristics like the drag ($\boldsymbol{C_d}$) and lift ($\boldsymbol{C_\ell}$) coefficients, recirculation downstream of the cylinder, average Nusselt number on the surface of the cylinder are presented and compared with previous results in the literature.

In this case, the angle formed by the segment joining the centers of the two cylinders and the abscissa axis is zero. For these simulations, a non-uniform mesh with $\boldsymbol{318 \times 164}$ point was used. The use of a uniform mesh in all computational domains, would considerably increase the computational cost. The simulation of flow develops from left to right. The velocity profile in the input field is uniform, with unit one value. In all simulations, the domain dimensions were $\boldsymbol{L_x = 55d}$ and $\boldsymbol{L_y = 30d}$. The cylinders were positioned at $\boldsymbol{x = 16.5d}$ and $\boldsymbol{y = 15d}$, where $\boldsymbol{d}$ represents the length of the side of the immersed body. For all simulations, a total of $\boldsymbol{201}$ points were used for the Lagragian mesh, with the non-uniform mesh in the region of the isothermal cylinder, maintaining a minimum amount of $\boldsymbol{30}$ meshes inside. For all simulations, the time step used in the calculation process was $\boldsymbol{10^{-6}}$, being dynamically calculated by the Courant-Friedrichs-Lewy (CFL) stability criterion, also known as CFL condition. To avoid numerical problems, the maximum grid expansion ratio of 3% was employed in these regions in both directions. In the present work, the ratio between the Lagrangian and Eulerian mesh sizes was maintained at 0.98. For the lateral boundaries of the domain, free boundary conditions were used, i.e., zero velocity at the border. At the entrance of domain, a velocity profile ($\boldsymbol{U_\infty}$) was imposed and, at the exit, the derivate is zero for the velocity. For the pressure, the boundary conditions used were Neumann at the entrance and Dirichlet at the exit, and on the sides of the sides of the domain, at the exit, and at the lower border were defined by $\boldsymbol{p = 0}$ and $\boldsymbol{\frac{\partial p}{\partial x} = \frac{\partial p}{\partial y} = 0}$.

For the temperature, the conditions are analogous, given by $\boldsymbol{\Theta = 0}$ and $\boldsymbol{\frac{\partial \Theta}{\partial x} = \frac{\partial \Theta}{\partial y} = 0}$. Concerning the initial condition, $\boldsymbol{u = v = 0}$, at $\boldsymbol{t = 0}$ (time), for the entrance computational domain. The cylinder is maintained at a constant dimensionless temperature equal to $\boldsymbol{1}$, i.e., $\boldsymbol{\Theta_c = 1}$; while the fluid has an initial temperature equal to zero. Although the boundary condition at the exit is not a reflective condition, the simulation results successfully support the formation of vortices outside the domain, without any reflection. The previously mentioned boundary conditions, at the entry and exit of the domain, are imposed, necessary to be consistent with the velocity, pressure and temperature equations, due to the grid arrangement chosen during the simulation. The total time duration in all simulations was 48h.

5.2 Calculation domain and Boundary conditions

In the Fig. (**1**), the two cylinders are identical and fixed with the same diameters, maintained in *tandem* (cylinders in line) with downstream of the cylinder A. The cylinders are confined to a channel with free flow, with uniform velocity ($\boldsymbol{U}_\infty$) and constant temperature $\left(\boldsymbol{T}_c(>\boldsymbol{T}_\infty)\right)$. The horizontal and vertical spacing between the cylinders are fixed in $\boldsymbol{L_u = 16.5d}$ and $\boldsymbol{L_d = 19.5d}$, respectively. These values are chosen to reduce the effect of boundary conditions on the inlet and outlet in relation to the flow pattern and cylinder contour.

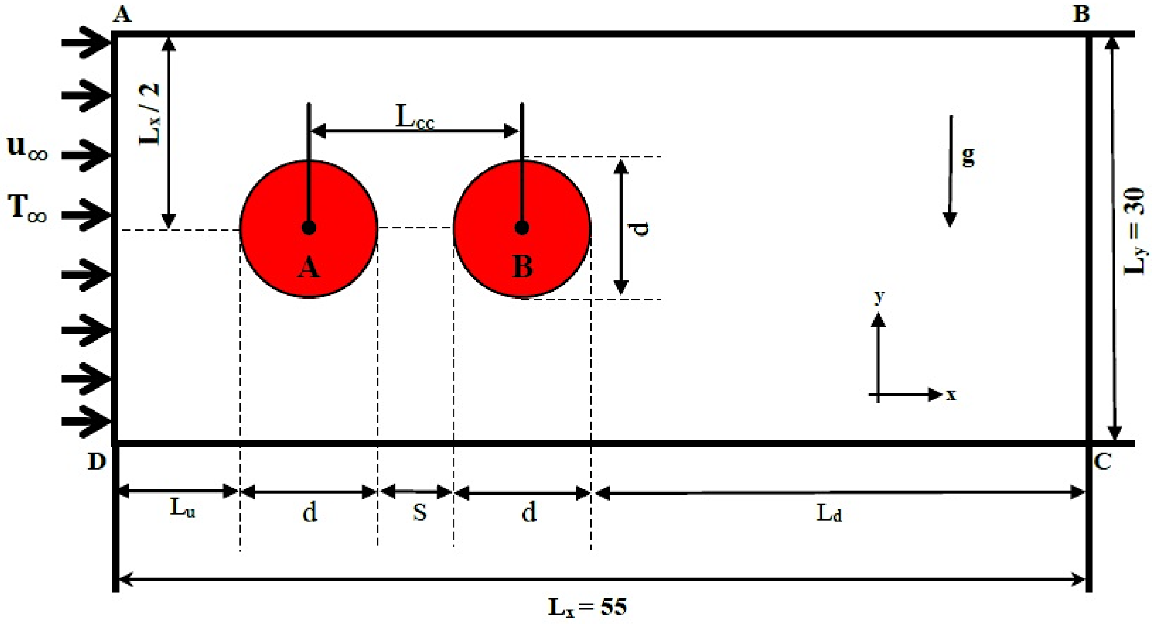

Figure 1: Illustration of the computational domain with two cylinders in tandem configuration.

The drag ($\boldsymbol{C_d}$) and lift ($\boldsymbol{C_\ell}$) coefficients for the calculation of each cylinder are performed as follows:

$$\boldsymbol{C_d = C_{dp} + C_{dv} = \frac{2F_d}{\rho U_\infty^2 D}}, \tag{19}$$

$$\boldsymbol{C_\ell = C_{\ell p} + C_{\ell v} = \frac{2F_\ell}{\rho U_\infty^2 D}}, \tag{20}$$

where, $C_{\ell p}$ and $C_{\ell v}$ represent the lift coefficients due pressure and viscous forces, respectively. In a similar way, C_{dp} and C_{dv} represent the drag coefficients due to the pressure and viscous forces. The terms, F_d and F_ℓ are forces of drag and lift, respectively, acting on the surface of the cylinder. Thus, the drag and lift coefficients can be obtained from the expressions:

$$\begin{cases} \boldsymbol{C_{dp}} = \mathbf{2}\displaystyle\int_{\mathbf{0}}^{\mathbf{1}} (\boldsymbol{p_f} - \boldsymbol{p_r})\boldsymbol{dy} \\ \boldsymbol{C_{dv}} = \dfrac{\mathbf{2}}{\boldsymbol{Re}}\displaystyle\int_{\mathbf{0}}^{\mathbf{1}} \left[\left\{\left(\frac{\partial \boldsymbol{u}}{\partial \boldsymbol{y}}\right)_s + \left(\frac{\partial \boldsymbol{u}}{\partial \boldsymbol{y}}\right)_i\right\}\boldsymbol{dx} + \left\{\left(\frac{\partial \boldsymbol{u}}{\partial \boldsymbol{x}}\right)_f + \left(\frac{\partial \boldsymbol{u}}{\partial \boldsymbol{x}}\right)_r\right\}\boldsymbol{dy}\right], \end{cases} \quad (21)$$

$$\begin{cases} \boldsymbol{C_{\ell p}} = \mathbf{2}\displaystyle\int_{\mathbf{0}}^{\mathbf{1}} (\boldsymbol{p_i} - \boldsymbol{p_s})\boldsymbol{dy} \\ \boldsymbol{C_{\ell p}} = \dfrac{\mathbf{2}}{\boldsymbol{Re}}\displaystyle\int_{\mathbf{0}}^{\mathbf{1}} \left[\left\{\left(\frac{\partial \boldsymbol{u}}{\partial \boldsymbol{y}}\right)_f + \left(\frac{\partial \boldsymbol{u}}{\partial \boldsymbol{y}}\right)_b\right\}\boldsymbol{dx} + \left\{\left(\frac{\partial \boldsymbol{u}}{\partial \boldsymbol{x}}\right)_t + \left(\frac{\partial \boldsymbol{u}}{\partial \boldsymbol{x}}\right)_i\right\}\boldsymbol{dy}\right]. \end{cases} \quad (22)$$

5.3 Simplified flow fields for $\boldsymbol{Re} = \mathbf{500}$ and $\boldsymbol{Ri} = \mathbf{0}$ to isothermal cylinders in tandem with forced convection

The Figs. (**2**) and (**3**), present simplified fields of temperature, pressure, effective viscosity, vorticity, isothermal lines, and aerodynamics coefficients, $\boldsymbol{C_d}$ and $\boldsymbol{C_\ell}$ for the flow around cylinders *in tandem*, for Reynolds and Richardson numbers, equals to 500 and 0, respectively.

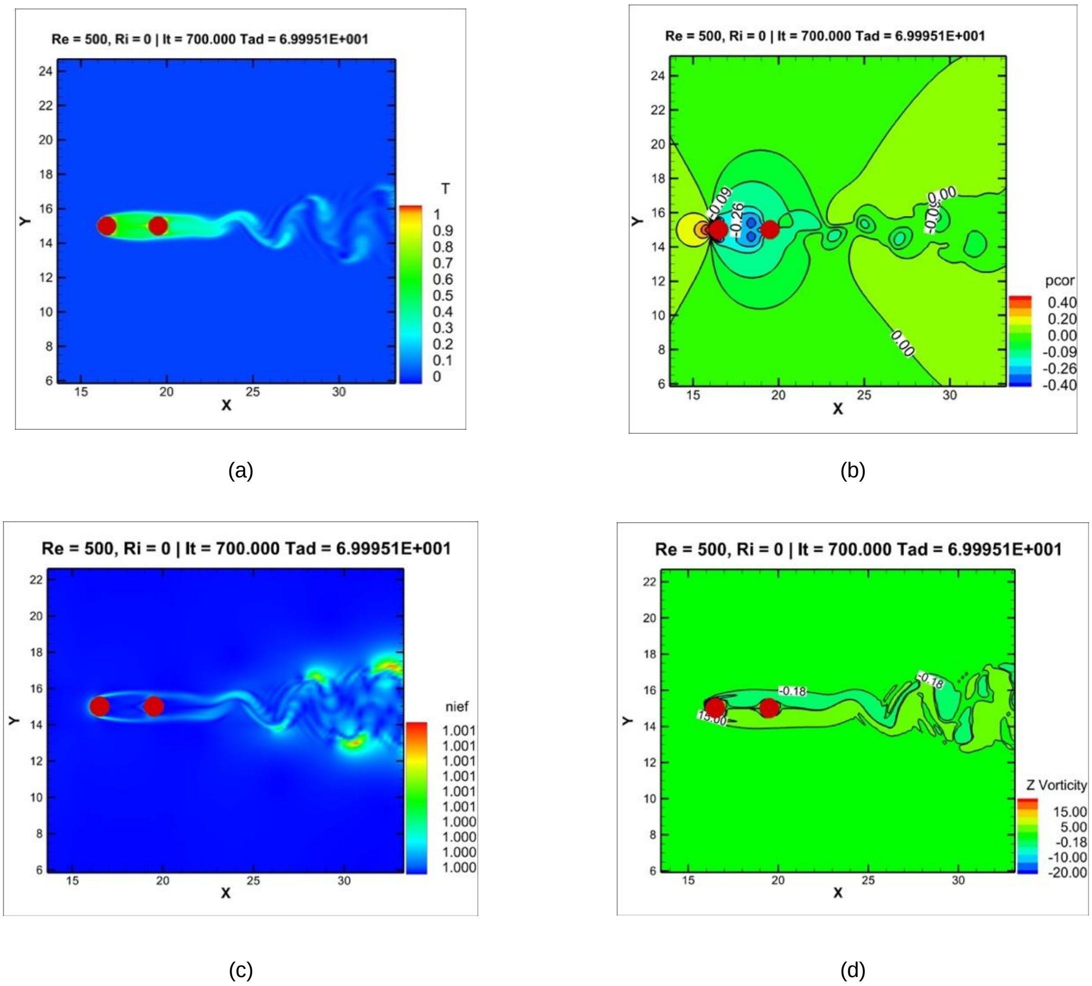

Figure 2: Smagorinsky model for simplified fields of (a) temperature, (b) pressure, (c) effective vorticity and (d) vorticity for $Re = 500$ and $Ri = 0$.

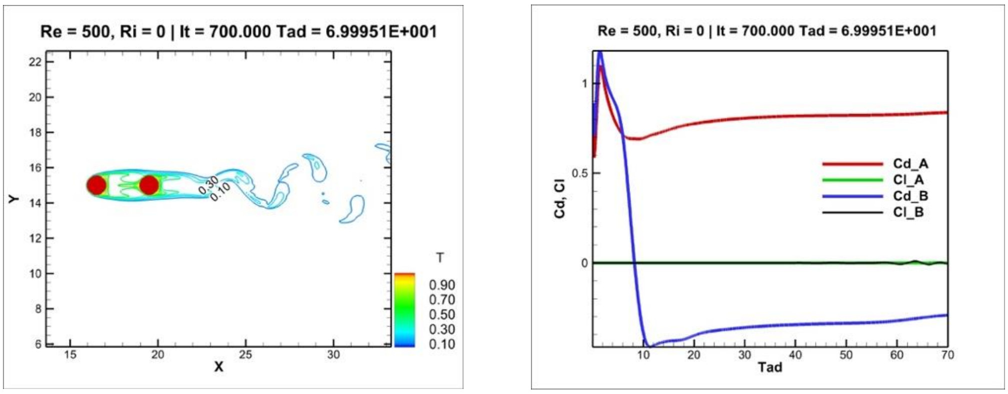

(e) (f)

Figure 3: Smagorinsky model for simplified fields of (e) isotherms lines and (f) drag and lift coefficients ($\boldsymbol{C_d}$, $\boldsymbol{C_\ell}$) for $Re = 500$ and $Ri = 0$.

The main results for the simulations can be summarized as follows:

- A wake forms upstream of the second cylinder, but it needs to be checked whether it can be decreased or suppressed with the increase of the distance between the cylinders;
- The isothermal lines reflect the same behavior of the pattern of the streamlines (current lines) – Fig. (**3**-(e));
- The thermal buoyancy is suppressed in the recirculation zones of the tandem cylinders, even with a mounting angle;
- The thermal buoyancy tends to in the recirculation zones of the tandem cylinders, even with a mounting angle.

6 Conclusions

This study presents the development of an immersed boundary method for simulating heat and mass transfer problems. The method accounts for the impact of thermal boundaries on the flow and temperature fields by applying velocity and temperature corrections. The temperature corrections are calculated implicitly to ensure the temperature at the immersed boundary conforms to physical boundary conditions. The method also incorporates a forcing term to account for momentum transfer between the immersed body and the surrounding fluid. To model onset turbulence, the Smagorinsky model, which is based on the local equilibrium hypothesis and the Boussinesq hypothesis, was utilized. A computational code was implemented to analyze the interaction of heat transfer and onset turbulence in thermofluid-dynamics around isothermal cylinders *in tandem*. The results were found to be in agreement with existing data in the literature, validating the effectiveness of the numerical method.

Conflicts of Interest: The author declares no conflict of interest regarding the publications of this paper.

References

1. Badr, H. M., & Dennis, S. C. R. (**1985**). Time-dependent viscous flow past an impulsively started rotating and translating circular cylinder. *Journal of Fluid Mechanics*, *158*, 447-488.
2. Badr, H. M., Coutanceau, M., Dennis, S. C. R., & Menard, C. (**1990**). Unsteady flow past a rotating circular cylinder at Reynolds numbers 10^3 and 10^4. *Journal of Fluid Mechanics*, *220*, 459-484.

3. Ashrafizadeh, A. and Hosseinjani, A. A. (**2017**). A Phenomenological Study on the Convection Heat Transfer around Two Enclosed Rotating Cylinders via an Immersed Boundary Method. *International Journal of Heat and Mass Transfer*, 107, 667-685.
4. Santos, R. D., Gama, S.M., & Camacho, R. G. (**2018**). Two-Dimensional Simulation of the Navier-Stokes Equations for Laminar and Turbulent Flow around a Heated Square Cylinder with Forced Convection. *Applied Mathematics*, 9(03), 291–312.
5. Santos, R.D.C. and Gama, S.M.A. (**2021**). Two-Dimensional Isothermal and Newtonian Flow in Complex Geometries. *Applied Mathematics*, 12, 91-129.
6. Silva, A. L. E., Silveira-Neto, A. and Damasceno, J. J. R. (**2003**). Numerical Simulation of Two-Dimensional Flows over a Circular Cylinder using the Immersed Boundary Method. *J. Comput. Phys.*, 189, 351–370.
7. Smagorinsky, J. (**1963**) General Circulation Experiments with the Primitive Equations: I. The Basic Experiment. *Monthly Weather Review*, 91, 99–164.

8. Schneider, G. E.; Zedan, M. A Modified Strongly Implicit Procedure for the Numerical Solution of Field Problems. *Numerical Heat Transfer*, v. 4, n.01, pp. 1-19, **1981**.